

AD-A082 767

TEXAS UNIV AT AUSTIN DEPT OF CHEMISTRY
AN ELECTRON SPECTROSCOPY STUDY OF AMMONIA ADSORPTION ON CLEAN Al₂O₃-ETC(U)
FEB 80 J W ROGERS, C T CAMPBELL, R L HANCE N00014-75-C-0922

F/0 7/4
NL

UNCLASSIFIED TR-12

[or]
AO
202Z7R7

END
DATE FILMED
5-80
DTIC

ADA082767

LEVEL

II

(12)

OFFICE OF NAVAL RESEARCH

Contract No. N00014-75-C-0922

Task No. NR 056-578

Technical Report No. 12

(6) An Electron Spectroscopy Study of Ammonia

Adsorption on Clean and Oxidized Aluminum

by

(10) J.W./Rogers, Jr. / C.T./Campbell, R.L./Hance and

J.M./White

Prepared for Publication

in

Surface Science

Department of Chemistry

University of Texas at Austin

Austin, Texas 78712

(11) February 29, 1980

Reproduction in whole or in part is permitted
for any purpose of the United States Government

Approved for Public Release; Distribution Unlimited



311,30 80 4 7 E 156

DDC FILE COPY

SECURITY CLASSIFICATION OF THIS PAGE (When Data Entered)

REPORT DOCUMENTATION PAGE		READ INSTRUCTIONS BEFORE COMPLETING FORM
1. REPORT NUMBER	2. GOVT ACCESSION NO.	3. RECIPIENT'S CATALOG NUMBER
4. TITLE (and Subtitle) An Electron Spectroscopy Study of Ammonia Adsorption on Clean and Oxidized Aluminum		5. TYPE OF REPORT & PERIOD COVERED Technical Report Jan. 1, 1980 - Dec. 21, 1980
7. AUTHOR(s) J. W. Rogers, Jr., C. T. Campbell, R. L. Hance and J. M. White		6. PERFORMING ORG. REPORT NUMBER N00014-75-C-0922
9. PERFORMING ORGANIZATION NAME AND ADDRESS J. M. White, Department of Chemistry University of Texas at Austin Austin, Texas 78712		10. PROGRAM ELEMENT, PROJECT, TASK AREA & WORK UNIT NUMBERS Project NR 056-578
11. CONTROLLING OFFICE NAME AND ADDRESS Department of the Navy Office of Naval Research Arlington, Virginia 22217		12. REPORT DATE February 29, 1980
14. MONITORING AGENCY NAME & ADDRESS (if different from Controlling Office)		13. NUMBER OF PAGES 46
		15. SECURITY CLASS. (of this report)
		16a. DECLASSIFICATION/DOWNGRADING SCHEDULE
16. DISTRIBUTION STATEMENT (of this Report) Approved for Public Release: Distribution Unlimited		
17. DISTRIBUTION STATEMENT (of the abstract entered in Block 20, if different from Report)		
18. SUPPLEMENTARY NOTES Preprint, accepted, Chemical Physics Letters.		
19. KEY WORDS (Continue on reverse side if necessary and identify by block number)		
20. ABSTRACT (Continue on reverse side if necessary and identify by block number) Photoelectron spectra for ammonia adsorbed in submonolayer and multilayer amounts on clean and oxidized aluminum have been measured and interpreted. Uptake at 128K is dominated by weak molecular adsorption and saturates at submonolayer amounts whereas at 106K multilayers can be formed. On oxidized Al, as compared to clean, the saturation amount of adsorbed NH ₃ is larger and it is more tightly held. On clean Al, there is good evidence that NH ₃ tends to be physisorbed with the major bonding arising between the permanent dipole of NH ₃ and the image dipole induced in the metal.		

DD FORM 1473 EDITION OF 1 NOV 68 IS OBSOLETE
1 JAN 73 S/N 0102-014-6601

SECURITY CLASSIFICATION OF THIS PAGE (When Data Entered)

Surface Sci. (in press).

2

Abstract

An Electron Spectroscopy Study of Ammonia Adsorption on Clean and Oxidized Aluminum

J.W. Rogers, Jr.^b, C.T. Campbell^c, R.L. Hance^d and
J.M. White
Department of Chemistry
University of Texas
Austin, Texas 78712

Photoelectron spectra for ammonia adsorbed in submonolayer and multilayer amounts on clean and oxidized aluminum have been measured and interpreted. Uptake at 128K is dominated by weak molecular adsorption and saturates at submonolayer amounts whereas at 106K multilayers can be formed. A tiny amount of dissociative adsorption is noted. Dissociation is promoted by exposure to Ar⁺ ion bombardment. At 128K the initial sticking coefficient is 0.13 ± 0.08 . On oxidized Al, as compared to clean, the saturation amount of adsorbed NH₃ is larger and it is more tightly held. In both cases the work function change is consistent with a model in which the ammonia adsorbs with the nitrogen atom toward the surface. On clean Al, there is good evidence that NH₃ tends to be physisorbed with the major bonding arising between the dipole of NH₃, and the image dipole induced in the metal. This is supported by the resemblance of the separation of the valence orbitals to the separation in the gas phase, as well as their shift to higher binding energy with increasing coverage. On oxidized Al the bonding is similar but the bond strength is greater. There is no evidence for significant NH₄⁺ formation on either clean or oxidized Al. The Lewis acidity of the substrate increases with the extent of surface oxidation. The bonding of NH₃ to oxidized Al is very similar to the intermolecular bonding in an ammonia molecular crystal.

a) Supported in part by the Office of Naval Research.
b) Present Address: Division 2516, Sandia Laboratories, Albuquerque, New Mexico 87185
c) N.S.F. Trainee, Present Address: Institut für Physikalische Chemie der Universität München, 8 München 2, West Germany.
d) Visiting Professor, Permanent Address: Department of Chemistry, Abilene Christian University, Abilene, Texas 79601.

1.1	Reaction/	Codes
Dist	Aval. and/or special	A

1. Introduction.

Alumina is an important catalyst support material and has intrinsic catalytic activity for certain reactions[1]. Being an ionic solid it has acid/base sites (Lewis and Brönsted-Lowry) associated with its surface cations and anions. The nature and behavior of these sites are of fundamental importance both in the presence and absence of dispersed metal particles.

Characterization of acidic sites on metal oxides has been studied using several techniques but direct spectroscopic data on the nature of such sites is scarce and much of our knowledge comes from inferences about the reactions that occur on them. Studies of bonding of gaseous bases to solid acid sites have been carried out using IR techniques [2,3,4,5,6]. Surface protonic sites, as well as the adsorption of deuterated pyridine on Brönsted sites, have been studied using NMR techniques [7,8,9].

Other techniques are discussed in reviews by Forni and Goldstein [10,11]. These techniques suffer from the two major disadvantages that the surfaces are usually not clean and well defined and that high pressures of the adsorbate gases are necessary to produce acceptable signal levels. In addition most of the techniques fail to differentiate between Lewis and Brønsted type acid sites, that is, they measure only total surface acidity.

XPS and UPS techniques, which probe electron levels within the adsorbate as well as bonds between the surface/adsorbate complex, should be ideal for the study of these interactions. Electron spectroscopic techniques have received little attention in examining surface acid sites because of experimental difficulties inherent with working on insulators. We have recently shown that charging

and thermal conductivity problems can be overcome by working with well characterized, selectively oxidized metal surface [12]. In addition, Hansen *et al.* have shown that oxidized Al surfaces model bulk Y-Al₂O₃ both physically and chemically [13].

Here we present an investigation of the interaction of NH₃ with clean and partially oxidized Al surfaces at low temperature using XPS and UPS techniques. XAES results from the same study have recently been published elsewhere [12] and the results are summarized here. In addition a characterization of the partially oxidized Al surfaces is presented. As inferred above, the motivation for this study comes from our desire to understand the molecular level details of the atomic and electronic structure of species chemisorbed on well-characterized metal oxides.

To contrast the differences in the behavior of NH₃ on clean and oxidized Al surfaces, it was first necessary to investigate the NH₃ interaction on clean Al. Electron spectroscopic studies of NH₃ adsorption have been reported on several metals including Fe [14,15,16,17], Cu[18], W[19,20], Ru[21,22], Mo[23,24] and Pd[25] as well as oxidized Cu[18]. Investigations of the interaction of NH₃ with metal oxides using these techniques are scarce [26].

2. Experimental Techniques.

The substrate was 1 cm² of 99.999% Al foil mounted such that it could be cooled to 106 K. The surface temperature was monitored with an attached chromel-alumel thermocouple.

The Al was initially difficult to clean; ~11h of Ar ion bombardment at 0.8 milliamp/cm² (5KV) at room temperature was required to remove the oxide layers as judged by XPS. Subsequent oxide layers acquired by overnight adsorption of residual gases or by O₂ exposure were removed with ~30 minutes of sputtering under the above conditions. Throughout this paper the Al will be called "clean" if the O(1s) integrated peak area was less than 5% of that observed for a monolayer. A monolayer, using the convention of Martinson et al.[27] is defined as the exposure necessary to produce an O(1s) peak area 90% of that at saturation. At 128 K this corresponds to an O₂ exposure of ~8L. Freshly sputtered Al was not annealed prior to exposure.

The experiments were performed on a PHI Model 548 Electron Spectrometer. The electron energy analyzer was operated in the retarding mode at a constant resolution of 0.4 eV (FWHM) for UPS and 1.6 eV for XPS. The surface was biased with a small negative voltage (3-6 volts) to facilitate accurate measurements of the kinetic energy distribution widths which were used to calculate the photoelectric work function [28]. All binding energies

were referenced to the Fermi level of Al; the Al(2s) BE for the clean surface was 117.6 eV, in good agreement with reported values [29].

The He resonance lamp, used for production of He I ($\hbar\omega=21.2$ eV) and He II ($\hbar\omega=40.8$ eV) photons, was differentially pumped.

The system base pressure, 2×10^{-10} Torr, rose to 1.2×10^{-8} Torr of 99% He when the line-of-sight valve into the UHV was open for UPS measurements. Mg(Kα) x-rays ($\hbar\omega=1253.6$ eV) were used for XPS measurements. NH₃ exposures were accomplished using a carefully calibrated, dynamically pumped doser system equipped with a multi-channel array which helped eliminate flux gradients across the sample[2]. An exposure of 50 L (1L=1 Langmuir= 10^{-6} Torr-sec) of ultra-pure NH₃ could be achieved in 13 minutes without raising the UHV system pressure above 1×10^{-9} Torr. Oxygen exposures were accomplished by backfilling the UHV system to no more than 2×10^{-7} Torr for a set amount of time. Residual and desorbed gases were monitored with a quadrupole mass spectrometer.

The XPS and UPS data were taken digitally using signal averaged pulse counting techniques and were stored in a multi-channel analyzer. A 20 eV wide energy window was typically scanned 16 times at a rate of 50 msec/channel and stored in 256 channels of memory. These could be permanently transferred to a magnetic tape on a CDC 6600 computer for subsequent manipulation.

3. Results.

3.1 The Characterization of Partially Oxidized Al Surfaces.

The O(1s) transition is plotted in Fig. 1 for several O₂ exposures at 128 K. The residual oxygen signal on "clean" Al always represented <5% of one monolayer of oxygen.

As noted in the UPS results below, this residual oxygen is probably dispersed in the bulk and therefore amounts to a small surface impurity. With increasing O₂ exposure a symmetric O(1s) peak is observed, the area of which grows until saturation after 159 L. The peak energy (531.3 eV) and FWHM (1.0 eV) do not change with exposure.

The O(1s) satellite from Ng K_O_{3.4} radiation, clearly present at higher exposures, is situated at ~522 eV.

The FWHM of the Al(2s) peak (not shown) grows from 2.5 eV on clean Al to 3.0 eV after 9 L exposure, and thereafter it remains constant. This is attributable to a shift of some intensity from 117.6 eV (Al⁰) toward 120.2 eV (Al³⁺) as the surface oxidizes [30].

Interestingly, condensing several multilayers of NH₃ on the oxidized surface caused the 2s intensity from oxidized Al at 120.2 eV to increase relative to the clean Al(2s) intensity at 117.6 eV, because the Al signal was coming from nearer the surface as the depth of NH₃ increased. This suggests that the oxygen resides primarily in the topmost several layers, which agrees with the general picture of the oxidation process [31,32,33]. The high signal

level, the instability of O₂ multilayer formation at these temperatures [34] and the lack of any attenuation of the Al(2s) transition, indicate that an appreciable amount of oxygen is being incorporated into the sub-surface region as previously reported [15,34].

Both the He I and He II UPS regions for the uptake of oxygen at 128 K are shown in Fig. 2. Curves a ($\hbar\omega = 21.2$ eV) and c ($\hbar\omega = 40.8$ eV) show the valence band of Al after sputter cleaning. The Fermi level is clearly present in both cases and BE's are referenced to it. The clean Al spectrum often showed a broad, low intensity peak centered near 7.1 eV due to emission from the O(2p) resonance (see Fig. 6). This peak derives from a small and variable amount of residual oxygen (~5% of a monolayer) which is detected with high sensitivity by UPS. The adsorption coefficient for 40 eV photons is twenty times greater for Al₂O₃ than Al [37]. Hagstrom, et al. have shown that ~0.01 monolayers of surface oxygen on Al can be detected by UPS [38].

The peak area in Fig. 2 grows rapidly with increasing exposure. After an exposure of 4.3 L, the Fermi level is no longer distinguishable because oxygen ions are formed and remove electron density from the valence band and because satellite peaks in He II add intensity just to the right of E_F in Fig. 2. The asymmetry of the O(2p) peak (FWHM = 6 eV) is discussed below. Curve 1 shows a low intensity transition near zero BE which is O(2p) emission caused by a He II satellite ($\hbar\omega = 48.31$ eV).

The He I region, shown at the left of the figure, is plagued by a high secondary electron background at low KZ which is caused in part by the analyzer transmission varying as KZ^{-1} in the retarding mode. On the cleanest Al surfaces, a narrow, low intensity peak is present at ~9.3 eV as seen in a. With increasing exposure, the intensity at 7.2 eV in He I grows faster than the 9.3 eV peak and becomes comparable to the intensity of the latter by ~1 L. After an exposure of 4.3 L the O(2p) resonances in He I and He II (spectra d and h) are indistinguishable in general peak shape.

The width and asymmetry of the O(2p) peak has been explained in terms of a superposition of two narrow transitions separated by 2.3 eV [30]. This interpretation suggests that O(2p) orbitals normal and parallel to the substrate have different BE for oxygen atoms in equivalent positions on the surface. Our results suggest that these two peaks are clearly resolvable in He I but not in He II because of an enhancement in the relative intensity of the 9.3 eV peak in He I. No more than 18% of this enhancement could be due to analyzer transmission. Since the electron escape depth is much larger in He I than in He II (20-30 Å [39] versus

$\sim 4 \text{ \AA}$ [40,41], we suggest that the 9.3 eV peak is characteristic of oxygen below the surface. This is to be compared with other assessments of the O(2p) splitting [42,43,44].

The integrated peak areas from the O(1s) and O(2p) ($\hbar\omega = 40.8 \text{ eV}$) regions as a function of oxygen exposure (at 128 K) are shown in Fig. 3. The coverage quickly rises to half its maximum value at an exposure of 2.5 L and continues to increase monotonically until it saturates at ~30 L. Using a first order Langmuir least-squares fit to the data and assuming saturation coverage = $5.2 \times 10^{14} \text{ cm}^{-2}$, an initial sticking probability $S_0 = 0.12$ was obtained.

Our purpose was to characterize the oxidized surfaces such that oxide-related intrinsic effects could be separated from the adsorbate-induced extrinsic effects accompanying NH₃ adsorption. The characterization was comprehensive enough to insure that the present results were in agreement with those previously reported in the literature. From the great body of information on Al oxidation the following picture of partially oxidized Al surfaces emerges:

1. At 0.9 L exposure, oxygen penetrates below the first layer of Al, producing a depletion layer rich in Al⁵⁺ as compared to clean Al [45,46].
2. Intermediate exposures of O₂ (4.3 L) produce a surface -75% covered by amorphous Al₂O₃ islands of thickness no greater than ~7 Å [30,33,36,38]. Patches of Al and Al⁶⁺ probably exist on this surface.

3. Heavy oxidation (260 L) leads to a 4-7 Å amorphous Al_2O_3 film covering the entire surface [30]. The observed behavior of NH_3 adsorbed on these oxidized surfaces is consistent with this picture.

3.2 The Interaction of NH_3 With Clean Al.

The N(1s) region for the adsorption of NH_3 on clean Al at 128 K is shown in curves a-e of Fig. 4. The spectra all exhibit a major peak near 400 eV, the area of which increases monotonically with increasing exposure. This is near the BE at which $\text{NH}_3(\text{ads})$ is expected based on NH_3 adsorption on other metals [14,15,16]. The FWHM of 3.0 eV remains constant as the exposure is increased, but the BE increases from 400.0 to 400.4 eV at exposures greater than 38 L which is close to saturation at 128 K.

A broad, low intensity peak at 396.2 eV is present even at the lowest exposures. The peak area, though difficult to determine accurately, does not appear to change with increasing NH_3 exposure. A ghost peak, originating from Cu(La) excitation of the Al(2p) transition, was only partially responsible for this feature.

A brief (90 sec.) exposure of the surface which produced curve e (maximum NH_3 adsorption at 128 K) to an Ar^+ ion beam causes a marked decrease in the intensity of the transition near 400 eV while increasing the intensity at 396 eV. This indicates the latter is produced by a dissociated nitrogen-containing species NH_{3-x} ($x = 1-3$). Probably $\text{N}(\text{ads})$. A $\text{N}(\text{ads})$ species with a BE at 397 eV has been reported on Al[32] and at 397 ± 0.5 eV on W and Fe[14,15,16,47] which lends further evidence to the present assignment. There is no evidence for NH_4^+ which would give a peak on the high BE side of the NH_3 signal.

Multilayer formation is not possible at 128 K and curve

e represents saturation coverage at this temperature. Spectrum f shows an NH₃ multilayer (58 L = 5 molecular layers) stabilised by lowering the surface temperature to 106 K. The width of the NH₃ multilayer peak in f (FWHM = 2.4 eV) is much narrower than that of the adsorbed NH₃ layer (FWHM = 3.0 eV) shown in e. The 0.6 eV broadening of adsorbate core levels with respect to the multilayer will be discussed below. A satellite peak near 391 eV in spectrum f is due to MgK_α3,4 radiation ($\hbar\omega = 1262.9$ eV) from the achromaticity of the X-ray anode.

An understanding of the molecular orbital structure and UPS spectrum of gas phase NH₃ is central to the assignment of photoemission peaks derived from adsorption of NH₃ on Al. The orbital representations of the valence levels for NH₃ showing contours of constant charge density [48] are presented in Fig. 5. From these diagrams it is apparent that the electrons in the 3a₁ orbital are predominantly non-bonding, while the 1e orbitals have high electron density centered between the N and H atoms and form the main N-H bonds.

The UPS ($\hbar\omega = 21.2$ eV) spectrum of NH₃ gas [49] is also shown in Fig. 5. The bands, whose maxima occur at 10.88 and 16.0 eV, arise from the 3a₁ and 1e orbitals respectively. The 1e⁻¹ transition is broad (FWHM = 2.2 eV) and exhibits a vibrational envelope. Interestingly, vibrational fine structure also appears in the non-bonding lone-pair 3a₁⁻¹ band. This is attributed to the NH₃⁺ ion being planar as opposed to NH₃ being trigonal bipyramidal; so despite non-bonding character of the 3a₁ orbital, it is important in

determining the NH₃ geometry [50,51].

The UPS ($\hbar\omega = 40.8$ eV) spectra for submonolayer coverages of NH₃ on clean Al at 128 K are displayed in Fig. 6. Curve a, showing the valence band of "clean" Al, is not identical with Fig. 2c, and indicates the variability of residual oxygen which we found. As seen in b-e, upon exposure to NH₃, two peaks are present centered at 6.3 and 11.8 eV; their peak areas increase with increasing exposure. The intensity at the Al Fermi edge is rapidly masked by a satellite peak produced from He II (3s + 1s) ($\hbar\omega = 48.31$ eV) excitation of the nitrogen orbitals which overlaps E_F.

The gas phase vertical ionization potentials are shown at the top of Fig. 6 after referencing them to E_F of Al by subtraction of the work function of the Al surface saturated with NH₃ at 128K [52]. On this scale, the 1e⁻¹ and 3a₁⁻¹ for gas phase ammonia occur at 13.9 and 8.4 eV, respectively. There is some uncertainty in the vertical ionization potential for the 1e orbital because the transition is broad and asymmetric. Here we have followed Grunze et al. [17] and have used the midpoint of the FWHM in Fig. 5. If instead, the typical method of using maxima is used, then the 1e⁻¹

would be placed at 13.5 eV. We favor the former largely because the latter leads to contradictory conclusions about the charge density on the nitrogen atom in adsorbed ammonia.

Comparing the gas and adsorbed phase spectra, it is clear that the symmetric features with maxima at 11.8 and 6.3 eV in the latter correspond to the gas phase $1e^{-1}$ and $3a_1^{-1}$ transitions respectively. Between 10 and 38 L, both these transitions shift to higher binding energy by about 0.4 eV. With respect to the gas phase, both adsorbed phase transitions are shifted to lower binding energy by 2.1 eV. We must obviously allow some uncertainty in these shifts, particularly in the case of the $1e^{-1}$. Regardless of this uncertainty the splitting of the adsorbed NH_3 on Al (5.5 eV) ^{is} more like the gas phase than it is on iron (4.4 eV) [17]. This fact suggests that chemical bonding of NH_3 , which on iron is thought to occur mainly through the lone pair of nitrogen, is largely absent in the case of Al. Another factor favoring weak bonding is the uniform shift to higher binding energy (0.4 eV) with coverage. This can be understood in terms of interactions between neighboring dipoles and their images [53]. This model gives a shift to higher binding energy because the permanent dipole of an ammonia molecule is stabilized through interactions with more than one image dipole. This attractive interaction is not fully compensated by repulsive interactions between dipoles.

A third observation favoring very weak binding of NH_3 to clean Al comes from warming experiments ($\text{N}(1s)$ versus T). Our results indicate a heat of adsorption of 9 ± 2 kcal mole⁻¹.

In spite of these considerations, there is one observation that suggests a stronger coupling of the lone pair orbital with the Al

surface than the N-H bonding orbital; namely, the branching ratio.

This quantity defined as the ratio of peak areas, $1e^{-1}/3a_1^{-1}$, is 2.0 for the gas [54] and 2.26 for the adsorbed phase [55]. Assuming that the $1e$ orbital is non-bonding and that the cross section for its ionization is comparable to the gas phase value, the $3a_1^{-1}$ intensity is clearly less than its gas phase analog suggesting a surface interaction with the lone pair which effectively removes some electron density from around the nitrogen atom. In the present case, this appears to be a redistribution spatially of the charge in the $3a_1^{-1}$ orbital rather than an actual loss of electron density. Accordingly, a shift of the $3a_1^{-1}$ binding energy to higher values is expected but not observed. One possible explanation is compensation due to more effective core-hole screening in the $3a_1^{-1}$ orbital due to its closer proximity to the surface. Calculations [56] indicate that differentials of a few tenths of an eV could be due to this source.

Taken together, all this evidence points to a very weak interaction of molecular NH_3 with clean Al surfaces resulting in a relaxation energy shift, ΔE_R , of 2.1 eV based on the position of the $1e^{-1}$ transition. While the $3a_1^{-1}$ shifts by the same amount, its intensity drops from gas phase values (relative to $1e^{-1}$) suggesting a slight redistribution of charge in this orbital as it interacts with the surface. We also find that work function changes (presented below) are consistent with the lone pair end of the NH_3 molecule toward the surface.

Comparison of UPS results for condensed and adsorbed NH_3 is perhaps even more informative than comparison of the latter with the gas phase results. Table I summarizes gas phase [49, 54, 57],

condensed [58], and the present physisorbed data. In passing from the physisorbed to the condensed phase the peak widths narrow 0.7 eV (FWHM). This is comparable to the 0.6 eV narrowing of the N(1s) core ionization noted above. Increased hole lifetimes in the multilayer can account for only a small part of this increase. For the case of a monolayer and multilayer of CO adsorbed on Cu [59,60] the observed decrease was 0.1 eV FWHM and this is in line with theoretical estimates [61]. The remaining 0.5 eV broadening in adsorbed NH₃ is tentatively ascribed to the range of work functions present on freshly sputtered polycrystalline Al. To the extent that the photoionization peaks should track the local vacuum level for physisorbed species [62,63] these peaks should broaden as much as the range of work functions available. Indeed it has recently been observed that the Xe levels broaden or even split when Xe is physisorbed on a partially reconstructed Ir(100) surface (where the work functions for reconstructed and unreconstructed Ir(100) both exist) [64]. This kind of heterogeneity-related broadening also explains why the NH₃ peaks we observe on Al are about 1 eV broader than those on Fe (111) [17].

From the linewidths and branching ratios presented in Table I, we are led to believe that the bonding of NH₃ in a condensed multilayer and a physisorbed monolayer is very similar. Cohesion in molecular crystals of NH₃ results from dispersion forces and weak hydrogen bonds [65,66]. As mentioned above we estimate from warmup measurements that the heat of adsorption of NH₃ on Al is 9 ± 2 kcal/mole whereas the heat of sublimation for NH₃ is 6.5 kcal/mole [67]. These facts are consistent with the notion that the Al

atoms involved in the NH₃ monolayer are similar to the H atoms in the NH₃ multilayer insofar as binding energetics and molecular orbital structures are concerned.

Spectrum b of Fig. 6 shows some additional intensity in the region between the $1s^{-1}$ and $3s^{-1}$ transitions not present in c, d and e. This is the region where features due to dissociated NH₃ have been reported on other metals [17,32] and we tentatively assign this intensity to NH_{3-x}(x = 1-3). However, we cannot rule out the possibility that it may be due to a small oxygen impurity.

The relative NH₃ coverage as a function of exposure, estimated by integrating the areas of the N(1s) peaks, is shown in Fig. 7. Also shown are the summed peak areas from the UPS He II region (Fig. 6). There is good agreement between the XPS and UPS data (normalized at 115 L). This is consistent with a relatively weak NH₃-Al interaction that involves very little charge transfer. In such a case the perturbation of the adsorbate valence levels is small and nearly coverage independent. Consequently the UPS intensity will reflect the adsorbate concentration.

The inset of Fig. 7 shows the work function change, $\Delta\phi$, as a function of NH₃ exposure at 128 K. These changes were determined by measuring the width of the photoelectron kinetic energy distribution. The measured work function of clean Al was $\phi_{Al} = 4.2$ eV. The results indicate a sharp decrease in work function accompanying increased NH₃ exposure up to 40 L at

which point the limiting change, $\Delta\phi = -1.7$ eV, is reached. The direction of the work function change is consistent with the nitrogen atom (electronegative end of the NH₃ dipole) being oriented toward the surface and the hydrogens toward the vacuum.

The coverage rises rapidly with NH₃ exposure reaching 80% of saturation at an exposure of 12 L and saturating with less than 60 L exposure. The saturation coverage can be estimated in a number of ways. Based on the absolute N(1s)/Al(2s) intensity ratio and using a method described in the literature [32,67], the saturation coverage N_{sat} is 8.6×10^{14} cm⁻². This estimate is expected to be high since significant Al(2s) intensity, appearing as intrinsic plasmon loss structure, is neglected. Using the relation for total work function change [68]:

$$\Delta\phi_{\text{sat}} = 4\pi eM N_{\text{sat}}$$

and approximating the dipole moment (M) of the adsorbate/surface complex with that of gaseous ammonia (1.47 Debye), we obtain N_{sat} = 3.2×10^{14} cm⁻². A close-packed monolayer of NH₃ (assuming r_{NH₃} = 1.53 Å) contains 1.4×10^{15} cm⁻². Saturation coverage at 128 K then corresponds to about 25 to 50% of a full monolayer. To estimate the initial sticking probability the data was least-squares fitted (solid line in the figure) to a first-order Langmuir adsorption equation of the form

$$\sigma = \{1 - \exp(-4.9 \times 10^{14} N_{\text{sat}}^{-1} S_0 L)\} . \quad (3)$$

where N_{sat} is the adsorbate surface density at saturation, S₀ is the initial sticking probability, L is the exposure (in Langmuirs)

and θ is the fractional coverage. Using N_{sat} = 5×10^{14} cm⁻² as an intermediate value, we obtain S₀ = 0.13. We must allow a factor of ± 0.08 to account for uncertainties in N_{sat}.

If the surface temperature is lowered to 106 K, NH₃ condensation is possible. Fig. 8 contrasts the adsorption of NH₃ at 106 K (triangles) and 128 K (circles from results in Fig. 7). The N(1s) peak area is plotted as a function of NH₃ exposure and the areas are normalized to the area of the Al(2s) transition obtained for clean Al prior to each NH₃ exposure. From measurements of the attenuation of the Al(2s) signal, the multilayer depth can be estimated at several coverages in Fig. 8. Assuming the thickness of an adsorbed NH₃ monolayer to be 3.05 Å (calculated from van der Waal's radii) and an Al(2s) attenuation length of 17 Å [39], the first monolayer occurs at a relative coverage of 0.9%. At 128 K, saturation coverage occurs near 0.3,

indicating that only 30% of the amount of NH₃ present in a monolayer at 106 K is stable on the surface at 128 K. This is in reasonable agreement with the estimates made above. The remaining data in Fig. 8 will be discussed below.

The uniform 0.4 eV binding energy shift with coverage of the N(1s) core and 1e and 3a₁ valence levels is noteworthy. As mentioned earlier, this can be understood in terms of long range image charge overlap [53]. Another possibility involves the question of whether adsorbate levels track the vacuum or Fermi level. This has been discussed by Kuppers et al. [64,69] who find similar effects in spectra of Xe on Pd(110). Physisorption on MoS₂ also exhibits these effects [62,63]. In weak adsorption systems adsorbate levels

are not in full electrochemical equilibrium with the substrate. As a result they do not precisely track the Fermi edge as is the case for chemisorbed systems. Rather they tend to track the vacuum level which changes with adsorbate induced work function changes.

The Ni_3/Al case is somewhere between the very weak physisorbed and fully chemisorbed cases; therefore, small shifts (~ 0.4 eV) with much larger changes in work function (1.7 eV) can be seen.

3.3. The Interaction of NH_3 on Partially Oxidized Al Surfaces.

The adsorption of NH_3 on Al surfaces pre-oxidized with 0.9, 4.3 and 260 L O_2 was studied at 128 K. These exposures represent low, half and saturation oxygen coverages at this temperature. The UPS and work function changes accompanying NH_3 adsorption as well as the temperature dependence of the adsorbate-derived XPS features indicate that, just as for clean Al, NH_3 is weakly held on oxidized surfaces; however, the interactions do differ significantly. The N(1s) core level transition appears at 400.3 eV as expected for molecular NH_3 adsorption and is equal to the BE observed for saturated NH_3 on clean Al at 128 K. As shown by the filled squares of Fig. 8 the capacity of the surface for adsorbing NH_3 increases with O_2 predose.

The UPS ($\hbar\omega = 40.8$ eV) features for the adsorption of NH_3 on oxidized Al surfaces are displayed in Fig. 9. As compared to clean Al, there are changes in the BE and intensities of the bands. To determine if the UPS features of NH_3 adsorbed on oxidized surfaces were simply superpositions of NH_3 and O_2 interactions on clean Al, the appropriate individual NH_3 and O_2 spectra were added, with scaling, to give good visual fits to the results obtained for NH_3 adsorbed on oxidized Al. The following procedure was used.

The digitized spectra for ammonia and for oxygen were (1) aligned at the He I Fermi level (not shown), (2) smoothed once with a five point quadratic/cubic smoothing algorithm, [70] (3) rescaled, (4) arithmetically summed, and (5) compared with the actual data from the oxidized surface. The scaling coefficients were varied and the procedure repeated until the best fit to the data (determined by inspection) was obtained.

The dotted curves in the figure show the scaled O(2p) intensity on clean Al at the indicated exposures and the dashed curves show the scaled NH₃ valence band for a 57 L exposure. The superpositions of these spectra are depicted by the dot-dashed curves and the solid lines show the actual data for NH₃ adsorption on oxidized Al. From the overall similarity of these, it is obvious that NH₃ exposures to oxidized Al at 128 K also produce molecularly adsorbed NH₃. This is in agreement with our XAES results [12] and XPS results discussed below. We will now discuss the slight differences that are observed in these two curves.

The scaling parameters, which accompany panels (A), (B) and (C) of Fig. 9 are summarized in Table II. Since the NH₃ exposure was fixed (58 L) the coefficient of the NH₃ dose indicates the amount adsorbed under each oxygen pre-dosed condition relative to clean Al. In each case the coefficient is greater than unity implying more NH₃ is adsorbed on oxidized Al. The XPS peak areas are in agreement with this observation as shown by the squares in Fig. 8. These results are all consistent with an increasing Lewis acidity with the extent of surface oxidation. An increased surface area would also tend to increase the amount of adsorbed NH₃, but photoelectron spectra and thermal stability experiments described below indicate that more than an area change is involved.

The oxygen scaling parameter represents the attenuation due to the NH₃ overlayer. As discussed above, exposure of Al to O₂ under the present conditions produces thin Al₂O₃ ($< 7 \text{ \AA}$) layers or islands even at exposures of 260 L. As seen in Table 2, the O₂ scaling factors decrease as the pre-oxidation exposure is increased. This indicates that the attenuation of the O(2p) signal by the NH₃ overlayer is greater for the thicker oxide films. This is expected since the oxide thickness, even for a 260 L exposure, is

no more than twice the mean free path of the O(2p) electron ($\lambda = 4 \text{ \AA}$ [40, 41]). Since a 0.9 L exposure of O₂ is completely incorporated just beneath the first layer of Al atoms without amorphous oxide formation, [45, 46], attenuation of the oxygen UPS signal by a monolayer of NH₃ is not expected (NH₃ diameter $\approx 3.04 \text{ \AA}$). However, as thicker oxide layers (but still $< 7 \text{ \AA}$ thick) are formed by O₂ exposures of 4.3 and 260 L, NH₃ adsorption should cause attenuation of oxygen derived UPS intensities as observed.

From inspection of Fig. 9, one can see that the NH₃ ($\tilde{\text{I}}_{\text{e}}^{-1}$) feature is shifted by 0.64 eV to higher BE when adsorbed on oxidized, as compared to clean, Al. A shift in this band could be due to a redistribution of charge in the N-H bonds as the result of hydrogen-bonding-like interactions with O²⁻ anions (see below, however). It is difficult to tell directly from Fig. 9 whether the ($\tilde{\text{I}}_{\text{e}}^{-1}$) transition is shifted on oxidized Al. However, by subtracting the scaled O(2p) resonance obtained on clean Al (dotted line), from the NH₃ covered oxidized Al surface (solid line), the resulting NH₃ features (not shown) indicate that the ($\tilde{\text{I}}_{\text{e}}^{-1}$) is also shifted by about 0.6 eV. The shift of both the $\tilde{\text{I}}_{\text{e}}^{-1}$ and $\tilde{\text{I}}_{\text{e}}'^{-1}$ transitions by similar amounts suggests that, compared to clean Al, core hole screening is less effective in the oxidized case. Campbell, et al. [58] found the same splitting of the $\tilde{\text{I}}_{\text{e}}^{-1}$ and $\tilde{\text{I}}_{\text{e}}'^{-1}$ orbitals in solid ammonia as has been observed for the gas phase (see Table I). Referenced to the Fermi level of Al, the BE's of solid NH₃ are shifted 2.5 \pm 0.1 eV to higher BE compared to those of NH₃ adsorbed on clean Al. A 0.64 eV shift to higher BE of the NH₃ levels following adsorption on oxidized Al, as well as the

absence of a significant differential shift between the $1e$ and $3a_1$ levels, suggests that the electronic environment of NH_3 in a solid molecular crystal and on an oxidized Al surface is similar. A shift of valence levels to higher BE has also been reported for CO adsorbed on oxygen-covered Pd [71]. Unfortunately, we can say nothing about how the peak widths change on oxidation due to uncertainties in the subtracted results.

The BE shift of the $(1e)^{-1}$ transition is smaller in curve (a) where a low O_2 exposure (0.9 L) leaves little oxygen on the surface. The behavior of the resulting Al^{6+} [45] surface to NH_3 adsorption should be similar to the clean Al surface except the bonding should be stronger due to the pre-existence of a permanent Al^{6+} dipole rather than the weak dipole induced by NH_3 adsorption on clean Al. These results are comparable to NH_3 physisorption on the Zn-rich face of ZnO (0001) which exhibits the same splittings as gas phase NH_3 [26, 72, 73]. However, NH_3 chemisorbs on ZnO at 246 K, and accompanying this strong interaction, the splitting between the $(1e)^{-1}$ and $(3a)^{-1}$ transitions is 2 eV less than the gas phase. Comparison with physisorbed NH_3 shows that the $(3a_1)^{-1}$ transition shifts with respect to the $(1e)^{-1}$ indicating a strong lone-pair interaction with the surface. Although NH_3 adsorption on oxidized Al and Zn is similar in many respects the bond energy on ZnO is significantly stronger. The limiting work function changes, $\Delta\phi$, for saturation coverages of NH_3 and O_2 on clean Al are -1.7 and $+0.2$ eV respectively. Adsorption of NH_3 on an oxidized (260 L O_2 /58 L NH_3) surface leads to a maximum $\Delta\phi$ of -0.5 eV (with respect to clean Al). Clearly the magnitude of $\Delta\phi$ on the oxidized as compared

to the clean Al surface, even taking into account the small positive work function change which occurs upon oxidation of Al, indicates the NH_3 dipole is significantly different on the two surfaces. The sign of the work function change is still consistent with the NH_3 overlayer having the negative end of the NH_3 dipole pointing toward the surface. One possible explanation for the reduced magnitude of $\Delta\phi$ on oxidized compared to clean Al is that the hydrogen atoms on NH_3 are being stabilized by neighboring surface oxygen anions. This is consistent with the UPS results mentioned above. It would tend to decrease the magnitude of the NH_3 dipole and result in a decreased work function change (compared to $\Delta\phi_{max}$ observed for NH_3 on clean Al). However,

we know of no good way to predict the work function change for this complex surface situation.

In light of the easy mobility of oxygen through the first few surface layers of Al, it is also possible that NH_3 adsorption induces changes in oxygen geometry and thereby work function changes unrelated to the NH_3 dipole.

In a separate set of experiments, the thermal stability of nitrogen-containing species were monitored using XPS of the $N(1s)$ ionization. The sample was saturated with NH_3 at 128 K and then warmed slowly by terminating the flow of liquid nitrogen to the cooling coils. A two-step decrease in the area of the $N(1s)$ peak at 400 eV with increasing temperature was observed indicating that roughly half the NH_3 desorbed at temperatures around 140 K. A small peak at 396 eV, assigned to adsorbed nitrogen atoms, was also observed.

I_{KV}S intensity increases during warmup to 200 K after which it declines. Characterization of the higher temperature species using thermal desorption and electron spectroscopic techniques warrants further investigation.

As noted earlier, XAES spectra of the N(KVV) region were taken for clean and oxidized Al surfaces saturated at 138 K with ammonia. The details are reported elsewhere [12]. By comparing the deconvoluted Auger spectra with gas phase [74,75, 76] and multilayer [77] spectra, perturbed NH₃ molecules are unmistakeably identified as the major adsorbed species. In agreement with the UPS and XPS data reported here, the XAES data suggest that the 3a₁ orbital is intimately involved in the interaction of NH₃ with the surface. The N(KVV) spectra for multilayer NH₃ and NH₃ adsorbed on oxidized Al are almost superimposable indicating the similarity in bonding in these two environments. Although the bonding is similar, the thermal stability and the saturation coverage increase with the level of surface oxidation, from which we conclude that the bond strength increases as the Lewis acidity of the surface increases.

4. Summary and Conclusions.

In this work UPS, XPS, XAES and work function change measurements have been used to characterize the adsorption and bonding of NH₃ on clean and pre-oxidized Al surfaces. Where possible, comparisons are made between gas, monolayer and multilayer spectra. The following conclusions are drawn:

- (1) At 128 K, ammonia adsorbs molecularly on both clean and oxidized aluminum. There may be a small amount of dissociative adsorption.
- (2) The saturation coverage at 128 K lies between 25 and 50% of a close-packed NH₃ overlayer.
- (3) The initial sticking coefficient at 128 K is 0.13 ± 0.08.
- (4) Multilayer formation is achieved by lowering the adsorption temperature to 106 K.
- (5) The thermal stability and extent of adsorption suggests that the NH₃ substrate bond is stronger on oxidized than on clean Al. This may arise because there is a fairly strong dipole-dipole interaction on oxidized Al whereas on clean Al the interaction involves dipole-induced dipole forces.
- (6) Unlike NH₃ on polar ZnO and Fe where there is a 2-3 eV differential shift of 3a₁ binding energies and unlike NH₃ ligands in organometallics where there is a strong dative bond, there is little shift of 3a₁ and only a weak physisorption bond in the case of NH₃ on Al and oxidized Al.
- (7) The bonding of NH₃ to an oxidized Al surface and in a condensed molecular crystal is similar.

(8) The Lewis acidity of an oxidized Al surface increases as the extent of surface oxidation increases.

(9) There is no evidence for an NH_4^+ type species on clean or oxidized surfaces.

Two observations emerged in this study which might be applied to other systems. The first, which was only briefly mentioned in the text, is the use of condensates to enhance surface sensitivity. Interesting heterogeneous catalytic chemistry generally occurs on the surface, not beneath it. Electron spectroscopy offers excellent surface sensitivity compared to other techniques, but the signal may still originate many atomic layers below the surface; the observed intensity is thus a combination of surface and bulk transitions. Preferential attenuation of the bulk signal by an inert, easily vaporized overlayer offers a powerful technique for determining, in a non-destructive fashion, interactions occurring within the first few atomic layers.

Secondly, UPS superposition techniques have been successful in separating intrinsic adsorbate effects from those extrinsically induced by the surface and vice versa. Sensible and useful information has been gained by interpreting the significance of scaling parameters used in the summation of spectra.

5. References.

1. S. Roy Morrison, "The Chemical Physics of Surfaces", New York: Plenum Press (1977), p. 333.
2. J. B. Peri and R. B. Hannan, J. Phys. Chem., 64, (1960) 1526.
3. H. Dunken, P. Fink and E. Pilz, Chem. Techn., 18 (1966) 490.
4. H. Dunken and P. Fink, Acta Chim. Acad. Sci. Hung., 53 (1967) 179.
5. J. B. Peri, J. Phys. Chem., 69 (1965) 231.
6. H. Dunken and P. Fink, Z. Chem., 5 (1965) 432.
7. W. K. Hall, H. P. Leftin, F. J. Chесelske, and D. E. O'Reilly, J. Catal., 2 (1963) 506.
8. R. M. Pearson, J. Catal., 23 (1971) 388.
9. R. M. Pearson, J. Catal., 46 (1977) 279.
10. L. Forni, Catal. Rev., 8 (1973) 65.
11. R. B. Anderson, "Experimental Methods in Catalytic Research", Volume 1, New York: Academic Press (1968), Chapter 9.
12. (a) J. W. Rogers Jr., Dissertation: An Electron Spectroscopic Investigation of the Interaction of Methanol and Ammonia With Clean Partially Oxidized Aluminum Surfaces, University of Texas at Austin, December 1979.
(b) C. T. Campbell, J. W. Rogers, Jr., R. L. Hance and J. M. White, Chem. Phys. Lett. (in press).
13. P. K. Hansma, D. A. Hickson and J. A. Schwarz, J. Catal., 48 (1977) 237.
14. F. Honda and K. Hirokawa, J. Electron Spectrosc. Relat. Phenom., 12 (1977) 313.
15. I. D. Gay, N. Textor, R. Mason, F. R. S. Iwasawa and Y. Iwasawa, Proc. R. Soc. Lond. A., 356 (1977) 25.
16. K. Kishi and M. W. Roberts, Sur. Sci., 62 (1977) 252.
17. M. Grunze, F. Bozzo, G. Ertl and M. Weiss, Appl. Sur. Sci., 1 (1978) 241.
18. M. H. Matloob and M. W. Roberts, Faraday Trans., 73 (1977) 1393.

19. P. J. Parrup and J. Anderson, J. Chem. Phys., **42** (1968) 523.
20. J. W. May, R. J. Szostak and L. H. Germer, Sur. Sci., **15** (1969) 37.
21. T. E. Maday and J. T. Yates, Jr., Proc. 7th Intern. Vac. Conf., 6th Intern. Conf. Solid Surfaces (Vienna, 1977), p. 1071.
22. L. R. Danielson, M. J. Dresser, E. E. Donaldson and J. T. Dickinson, Sur. Sci., **71** (1978) 599.
23. T. Kawai, K. Kunimori, T. Kondow, T. Onishi and K. Tamaru, Phys. Rev. Lett., **33** (1974) 533.
24. T. Kawai, K. Kunimori, T. Kondow, T. Onishi and K. Tamaru, Proc. 2nd Intern. Conf. on Solid Surfaces (Koyoto, 1974), Japan J. Applied Phys. Suppl., **2** (1974) 513.
25. K. Kunimori, T. Kawai, T. Kondow, T. Onishi and K. Tamaru, Sur. Sci., **59** (1976) 302.
26. R. R. Gay, I. E. Solomon, V. E. Henrich and H. J. Zeiger, Thirty-Eighth Annual Conf. on Physical Electronics (Oak Ridge, Tenn., 1978), unpublished.
27. C. W. B. Martinsson and S. A. Flodstrom, Sur. Sci., **80** (1979) 306.
28. J. A. Connor, M. Considine, I. H. Hillier and D. Briggs, J. Electron Spectrosc. Relat. Phenom., **12** (1977) 143.
29. J. W. Robinson, "Handbook of Spectroscopy", Cleveland, CRC Press (1974) Vol. 1, p. 518.
30. S. B. M. Hazstrom, R. Z. Bachrach, R. S. Bauer and S. A. Flodstrom, Physica Scripta, **16** (1977) 414.
31. E. E. Huber, Jr. and C. T. Kirk, Jr., Sur. Sci., **5** (1966) 447.
32. A. F. Carey and M. W. Roberts, Proc. Roy. Soc. London A, **363** (1978) 403.
33. J. C. Fuggle, L. M. Watson, D. J. Fabian, and S. Affrossman, Sur. Sci., **49** (1975) 6.
34. P. Hofmann, K. Horn, A. M. Bradshaw, and K. Jacob, Sur. Sci., **82** (1979) 1610.
35. P. Hofmann, W. Myrbisch and A. M. Bradshaw, Sur. Sci., **80** (1979) 344.
36. P. O. Gartland, Sur. Sci., **62** (1977) 183.
37. H. J. Hagemann, W. Gudat and C. Kunz, Deutsches Elektronen-Synchrotron, DESY SR-7/7, May 1979.
38. S. A. Flodstrom, R. Z. Bachrach, R. S. Bauer and S. B. M. Hazstrom, Proc. 7th Intern. Vac. Conf., Solid Surfaces (Vienna, 1977), p. 865.
39. F. L. Battye, J. G. Jenkins, J. Lieseberg and R. C. G. Leckey, Phys. Rev. B, **9** (1974) 2887.
40. C. J. Powell, R. J. Stein, P. B. Needham, Jr. and T. J. Driscoll, Phys. Rev. B, **16** (1977) 1370.
41. A. Bianconi, R. Z. Bachrach and S. A. Flodstrom, to be published.
42. J. R. Chelikowsky, M. Schluter, S. G. Louie and M. L. Cohen, Solid State Commun., **17** (1975) 1103.
43. J. Harris and G. S. Painter, Phys. Rev. Lett., **36** (1976) 151.
44. N. D. Lang and A. R. Williams, Phys. Rev. Lett., **37** (1976) 212.
45. K. Y. Yu, J. N. Miller, P. Chye, W. E. Spicer, N. D. Lang, and A. R. Williams, Phys. Rev. B, **14** (1976) 1446.
46. M. W. Roberts and B. R. Wells, Sur. Sci., **15** (1966) 325.
47. T. E. Maday, J. T. Yates, Jr. and N. E. Erickson, Sur. Sci., **43** (1974) 526.
48. W. L. Jorgenson and J. Salem, "The Organic Chemist's Book of Orbitals", New York: Academic Press (1973) 69.
49. Our thanks to Mike Lattman for running the gas phase NH₃ spectrum. This spectrum agrees well with published results (see 50,51 and A. W. Potts and W. C. Price, Proc. Roy. Soc. (London) A326 (1972) 181.)
50. J. H. D. Eland, "Photoelectron Spectroscopy", London: Butterworths (1974) 112.
51. J. W. Rabalais, "Principles of Ultraviolet Photoelectron Spectroscopy", New York: Wiley Interscience (1977) 251-255.
52. H. D. Hagstrum, Sur. Sci., **54** (1976) 197.
53. G. Doyen, J. Kuppers, F. Nitschke, K. Wandelt and G. Ertl (to be published).
54. D. A. Allison and R. G. Cavell, J. Chem. Phys., **68** (1978) 593.
55. The gas phase branching ratios were taken from reported He II ($\lambda_{\text{W}} = 40.8 \text{ eV}$) literature values to ensure that cross-sections for ionization in the gas and adsorbed phases were identical. The substrate contributions were subtracted from curve **e** (Fig. 5) before integrating and the resulting areas were corrected for analyzer transmission.

56. P. R. Antoniewics (*private communication*).
 57. C. E. Brion, A. Hamnett, G. R. Wright and M. J. Van Der Wiel, *J. Elect. Spectrosc. Relat. Phenom.*, 12 (1977) 323.
 58. M. J. Campbell, J. Liesegang, J. D. Riley, R. C. G. Leckey and J. C. Jenkin, *J. Elect. Spectrosc. Relat. Phenom.*, 15 (1979) 83.
 59. P. R. Norton, R. L. Tapping, H. P. Broida, J. W. Gadzuk, and B. J. Waclawski, *Chem. Phys. Lett.*, 53 (1978) 465.
 60. P. R. Norton, R. L. Tapping and J. W. Goodale, *Sur. Sci.*, 22 (1978) 33.
 61. M. O. Kruse, *J. Phys. Chem. Ref. Data*, 8 (1979) 307.
 62. K. J. Yu and J. C. McMenamin and W. E. Spicer, *Surf. Sci.*, 50 (1975) 149.
 63. K. J. Yu, W. E. Spicer, I. Lindau, P. Pianetta and S. F. Lin, *Surface Sci.*, 57 (1976) 157.
 64. J. Kuppers, H. Michel, F. Nitschke, K. Wandelt and G. Ertl, *Surf. Sci.*, 89 (1979).
 65. G. C. Pimentel, and A. L. McClellan, "The Hydrogen Bond", San Francisco: Freeman (1960).
 66. L. Pauling, "The Nature of the Chemical Bond", Ithaca, N.Y.: Cornell Univ. Press (1939).
 67. T. E. Madey, J. T. Yates and M. E. Erickson, *Chem. Phys. Lett.*, 19 (1973) 487.
 68. R.B. Anderson, Ed., "Experimental Methods in Catalytic Research", New York: Academic Press (1968) 104.
 69. J. Kuppers, F. Nitschke, K. Wandelt and G. Ertl, *Surface Sci.*, 88 (1979) 1.
 70. A. Savitzky and M. J. E. Golay, *Anal. Chem.*, 36 (1964) 1627.
 71. H. Conrad, G. Ertl and J. Kuppers, *Sur. Sci.*, 76 (1978) 323.
 72. R. R. Gay, E. I. Solomon, V. E. Henrich and H. J. Zeiger, unpublished.
 73. R. R. Gay, E. I. Solomon, V. E. Henrich and H. J. Zeiger, *Newsletter, Amer. Chem. Soc., Div. Inorg. Chem.*, January, 1978.

TABLE II
Scaling Factors for Ammonia on Pre-oxidized Aluminum

	Oxygen Pre-dose		
	0.9 L	4.3 L	260 L
Scaling factor for oxygen features	1.0	0.8	0.7
Scaling factor for NH ₃ features ^a	1.1	1.1	1.4
Ratio of N(1s)[oxidized]/N(1s)[clean] ^b	1.8	1.8	2.3

^aFrom Fig. 9^bFrom Fig. 8

The saturation coverage at saturation NH₃ coverage has been subtracted from the reported literature values to facilitate comparison with the present work ($\phi_{Al} + \phi_{NH_3} = 2.5$ eV). The work function at saturation NH₃ coverage was not reported in Ref. 58 but we assume that it was at least better than $\Delta E(FWHM) = 0.4$ eV since the work was done in the gas phase.

Saturation coverage (115 L exposure) at 128 K.

All energies are reported in eV.

Speculum	Gaseous NH ₃		Solid NH ₃		Adsorbed NH ₃		Parameters ^a		Binding Energies ^c		Wavelengths		Energy Bandwidths		Separation Energy		Branching Ratios [e/3a]		
	3a ₁	1e	1a ₁	3g ₁	1e	3g ₁	1e	1e	0.38 [49]	13.3 [49]	403.5 [51]	8.8 [58]	14.2 [58]	6.3	11.8	400.4	--	2.0 [54]	--
									1.7 _d [57]	2.5 [57]	--	1.8 [57]	3.0 [58]	2.6	3.7	--		5.12 [49]	--
												5.4 [58]		3.5				2.18 [58]	2.29

TABLE I Electron Spectroscopic Parameters for Ammonia

TABLE I

Figure Captions.

Figure 1. O(1s) spectra for various exposures of polycrystalline Al to O_2 at 128 K. Mg K α x-rays at 1253.6 eV.

Figure 2. He I and He II photoelectron spectra for oxygen chemisorbed on polycrystalline Al at 128 K. Note different intensity scales for the two panels.

Figure 3. Peak areas for oxygen valence (0) by UPS and core 1s (A) by XPS photoionizations as a function of oxygen exposure at 128 K. Solid line is a fit to a first order adsorption model.

Figure 4. N(1s) core level XPS spectra for various exposures of NH_3 on polycrystalline Al. Spectra 4-e involve exposure at 128 K. Spectrum f is a multilayer built up at 106 K.

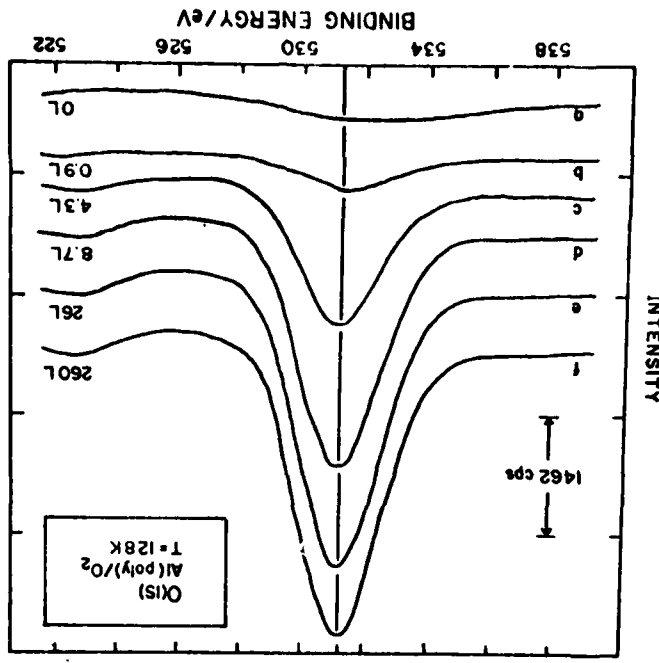
Figure 5. Gas phase UPS/ammonia [49] and representations of valence molecular orbitals of NH_3 showing contours of constant charge density. (Reproduced from reference 48 with permission.)

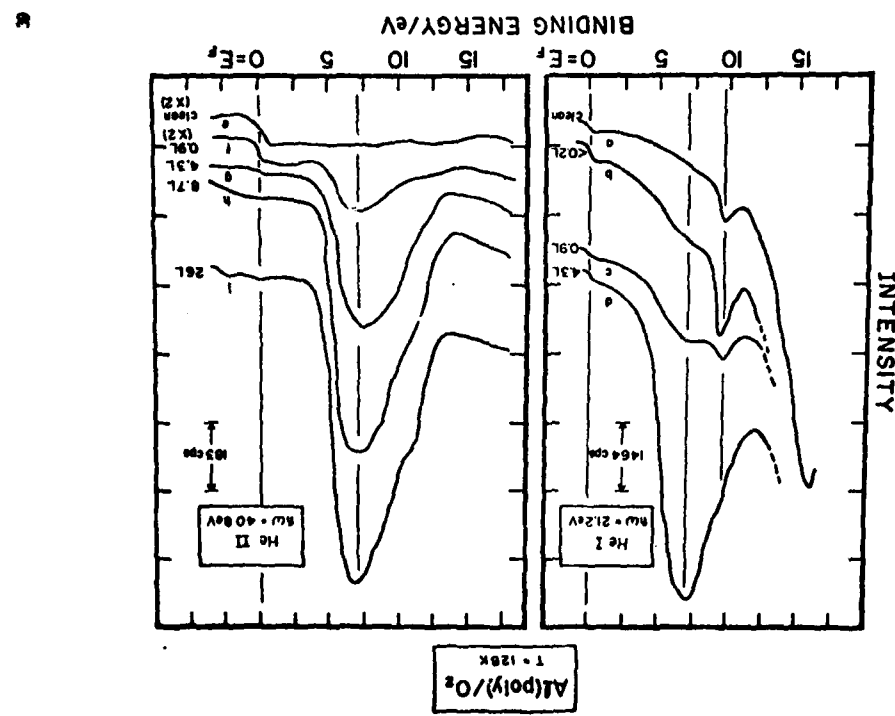
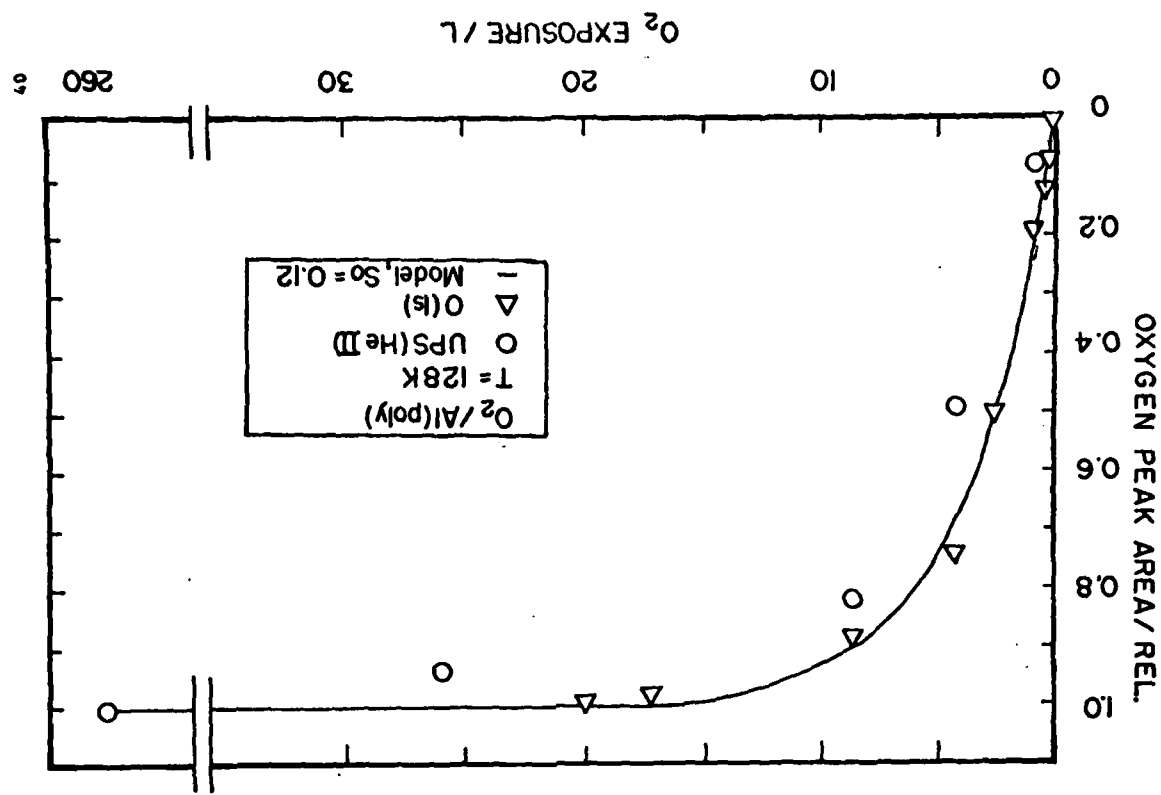
Figure 6. UPS (He II) spectra for various exposures of NH_3 on polycrystalline Al at 128 K. The gas phase ionization potentials (see text) are shown at the top.

Figure 7. Peak areas as a function of exposure at 128 K for the x-ray excited N(1s) core level (Δ) and the He II valence levels (○) of ammonia adsorbed on polycrystalline Al. The solid line is a fit to a first order Langmuir adsorption model with an initial sticking coefficient of 0.13 (see text). The inset shows the change in work function with ammonia exposure. This was determined using the widths of He II spectra.

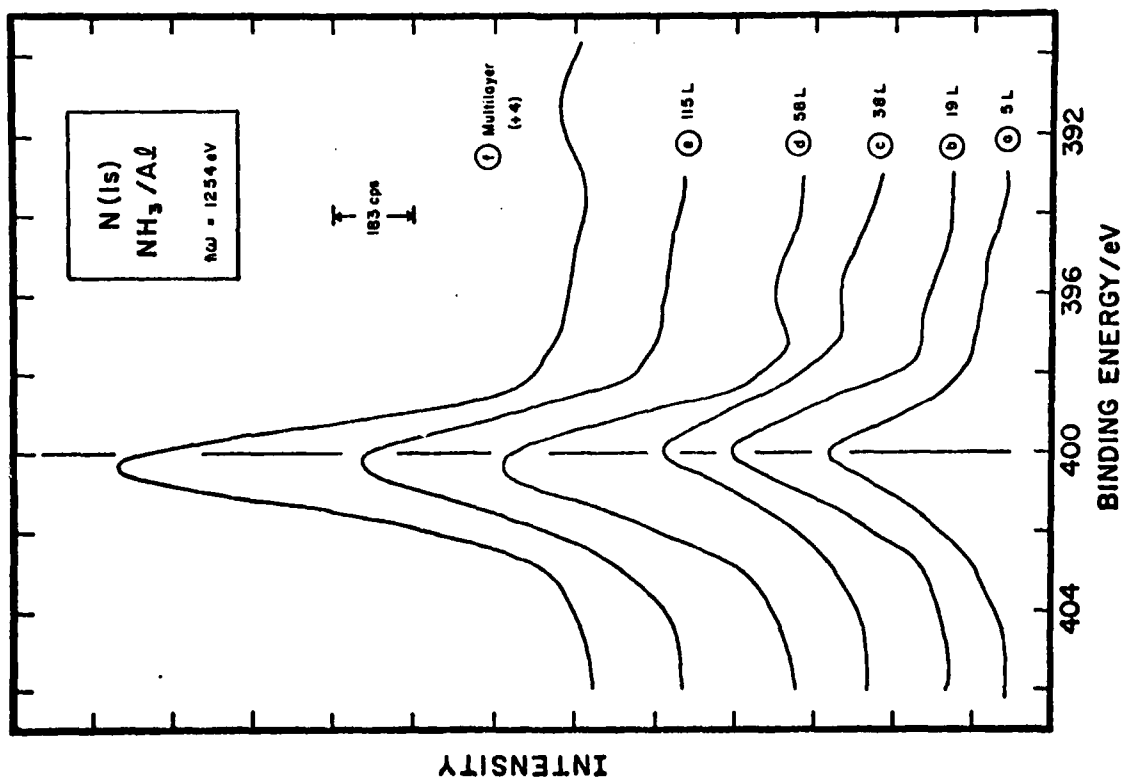
Figure 8. N(1s) peak areas, normalized to the Al (2s) peak area for a surface free of ammonia, versus exposure at 128 K (○) and 106 K (▲). The filled squares show the same quantity, determined at 128 K, for Al predosed in O_2 , at three different exposures followed by a 58 L exposure to NH_3 .

Figure 9. He II spectra for NH_3 adsorbed on oxidized Al at 128 K. Solid curve is actual UPS spectrum. Dotted curve is a scaled spectrum of oxygen alone on Al. Dashed curve is a scaled version of NH_3 alone on Al. Dot-dashed curve is sum of the two scaled spectra. A involves a predose of 0.9 L O_2 followed by 58 L NH_3 , B is for 4.3 L O_2 and 58 L NH_3 while C is for 260 L O_2 and 58 L NH_3 .

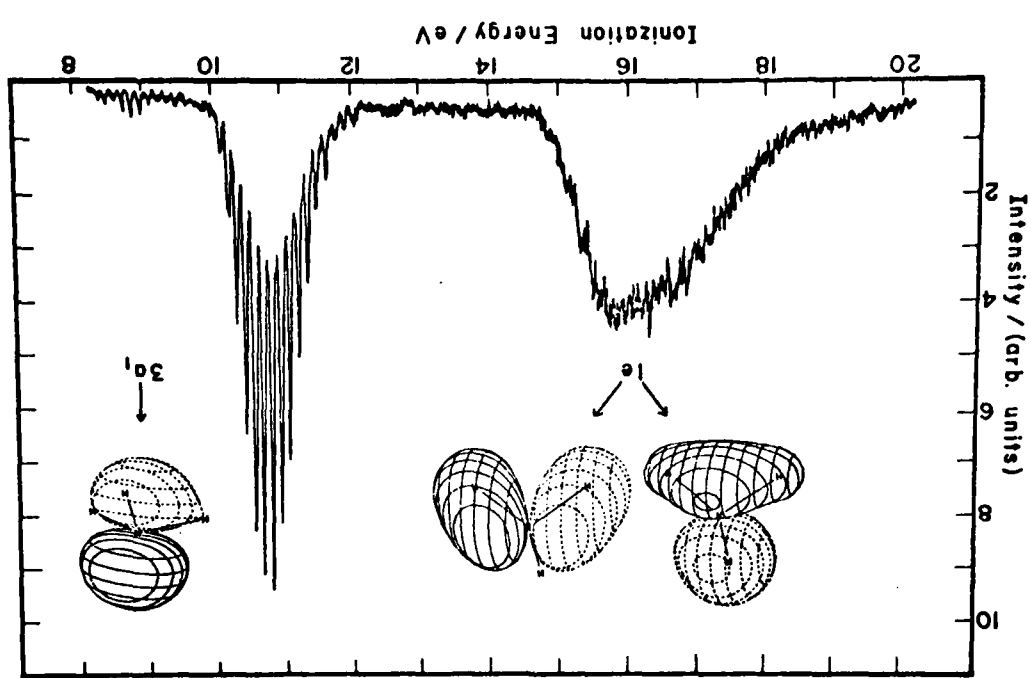




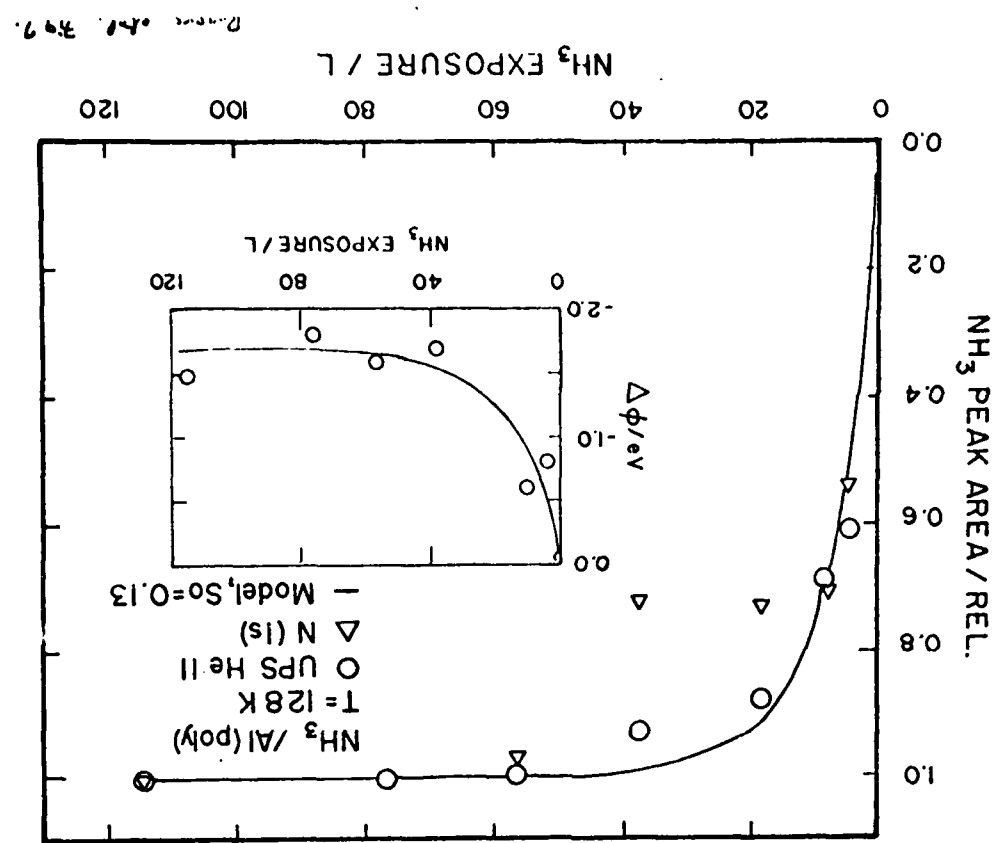
41



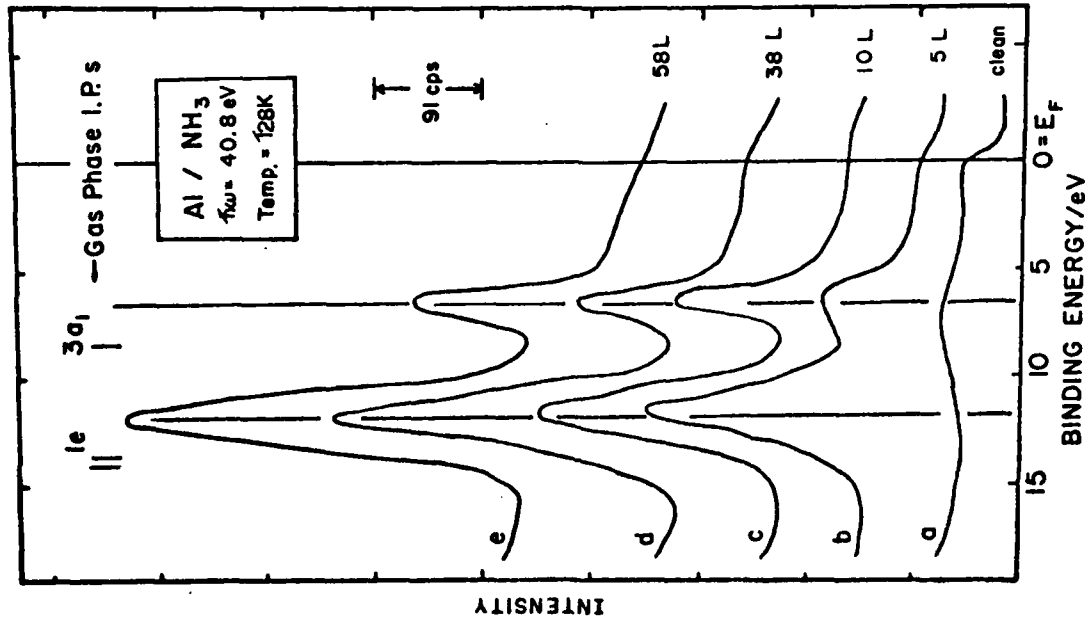
42

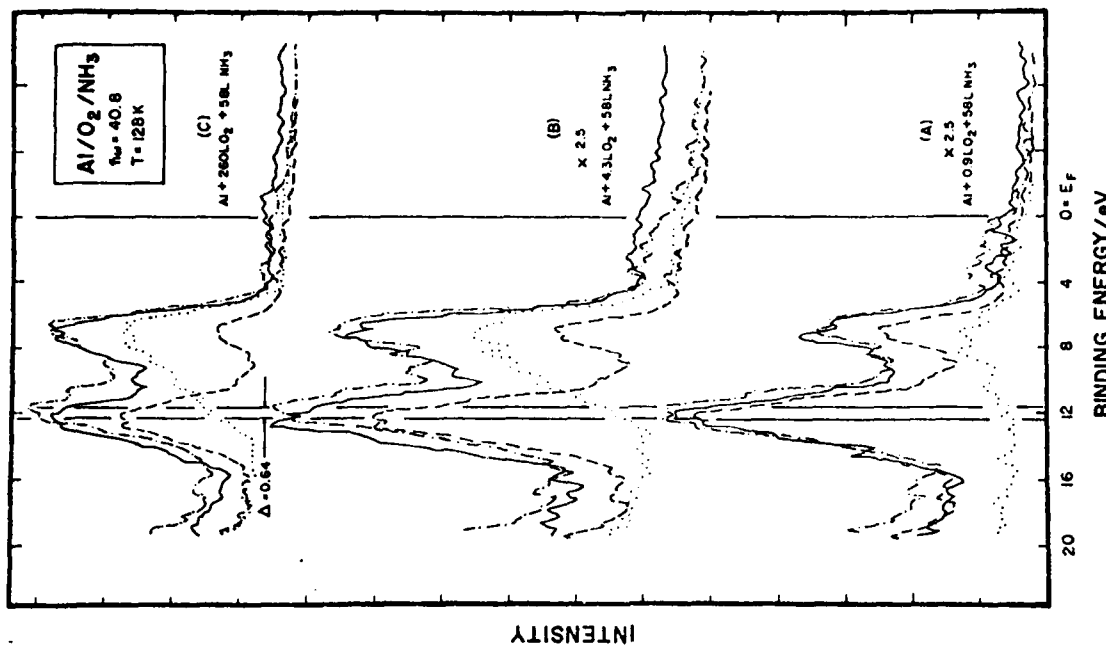


44



43





Ragno et al. 778

